New NADPH/9-AA module for the DUAL-PAM-100: Description, operation and examples of application.

Ulrich Schreiber and Christof Klughammer

Abstract

The NADPH/9-AA module has become available as a new accessory for the DUAL-PAM-100. Fluorescence is excited at 365 nm using a UV-A Power LED. A photomultiplier sensor is employed for detection of blue-green emission (420 to 580 nm). The new module was optimized for measuring light-induced changes of NADPH fluorescence in suspensions of isolated chloroplasts, algae and cyanobacteria. It also may serve for highly sensitive measurements of various fluorescent probes, like 9-amino-acridine (9-AA), 9-amino-6-chloro-2-methoxyacridine (ACMA), acridine orange and acridine yellow, which in the past have been used for non-invasive monitoring of bioenergetic processes in isolated chloroplasts and whole cells. Technical features of the new emitter-detector module are outlined and some hints for optimal use of the new device and of the Dual-PAM software are given. Examples of application are focused on the phenomenology and interpretation of light induced NADPH fluorescence changes in suspensions of isolated spinach chloroplasts, *Chlorella vulgaris* and cyanobacteria (*Synechococcus* PCC 7942 and *Synechocystis* PCC 6803). Also simultaneous measurements of chlorophyll (Chl) and NADPH fluorescence are presented, revealing parallel and anti-parallel kinetic phases. Under favorable conditions, Saturation Pulses can serve for estimating the extent of NADP reduction in the steady state.

Introduction

Duysens and Amesz (1957) first measured NADPH emission spectra in photosynthetic bacteria. Olson (1958) presented first kinetic recordings of dark-light-dark induced NADPH changes in *Rhodospirillum*, *Anacystis* and *Chlorella*. Cerovic *et al*. (1993) measured simultaneously Chl and NADPH dark-light fluorescence induction in isolated chloroplasts employing a pulse-modulated nitrogen laser. Detailed kinetics in dependence of various metabolic factors was presented at 1-10 Hz time resolution.

Mi *et al*. (2000) studied NADPH fluorescence *in Synechocystis* PCC 6803 and its ndhB-defective mutant M55 with a PAM fluorimeter and a special Emitter-Detector unit at 100 KHz time resolution. Using repetitive illumination at saturating intensity, the observed transients revealed highly complex dynamic changes reflecting the interplay of various metabolic pathways involving NADPH and NADH.

While this previous work has demonstrated the potential of NADPH measurements, up to now this tool has been rarely applied, due to the small signal amplitude and the lack of commercially available, easy to handle instrumentation. Here we report on a new NADPH/9-AA module for the DUAL-PAM-100, application of which is greatly facilitated by a powerful user software that has been specifically extended for the sake of NADPH measurements.

The new module employs pulse-modulated UV-A excitation light (365 nm) for measuring either NADPH/NADH or 9-aminoacridine (9-AA) fluorescence in suspensions of isolated chloroplasts, unicellular algae or cyanobacteria. Both signals can be measured simultaneously with Chl fluorescence. While NADPH fluorescence changes provide information on electron transport at the acceptor side of Photosystem I (PS I), 9-AA fluorescence quenching may serve as an indicator of the transthylakoid membrane proton gradient (ΔpH).

The DUAL-PAM-100 was designed as a modular measuring system with the possibility to measure one pulse-modulated *single beam signal* (normally Chl fluorescence excited by red or blue measuring light) and one pulse-modulated *dual beam difference signal* (normally P700 absorbance detected via the difference in transmittance of 870 and 830 nm light). Alternatively, also *two single beam signals* can be measured. The Emitter-Detector units for measuring Chl fluorescence and P700 can be readily exchanged against alternative Emitter-Detector units that have been developed for assessment of other types of optical changes that may provide complementary information on photosynthesis.

In a preceding communication, Schreiber and Klughammer (2008) already reported on the P515/535 module, which allows simultaneous measurements of the electrochromic pigment shift (ECS, P515) and of "scattering" changes reflecting "membrane energization". In this way, the DUAL-PAM-100 has been continuously evolving into a universal measuring system for profound non-invasive analysis of photosynthesis.

Some background on fluorescence from NADHP, 9-AA and other fluorescent probes

NADPH fluorescence

NADPH fluoresces in the blue-green spectral region in contrast to NADP, which does not fluoresce. The excitation spectrum of NADPH fluorescence shows a maximum in the UV-A region around 340 nm. The emission

peaks around 465 nm. Measuring NADPH fluorescence in photosynthesizing organisms is complicated by a number of facts that so far have prevented widespread application of this tool:

a. The amplitude of NADPH fluorescence is about 2000 times smaller than that of Chl fluorescence (using identical 365 nm excitation).

b. The UV excitation light is not only absorbed by NADPH, but also by numerous other cell constituents, including photoprotective and photosynthetic pigments.

c. Non-NADPH excitation (of cellulose, flavins etc.) gives rise to a "background signal" that may be several fold larger than the NADPH signal.

d. NADPH accumulates at very low light intensities, making the use of high measuring light intensity problematic.

e. The blue-green emission is efficiently reabsorbed by photosynthetic pigments, thus preventing use of high Chl concentration (with correspondingly high NADP content).

As will be shown in this communication, despite of these unavoidable complications, the specifications of the DUAL-PAM-100 and of the newly developed NADPH Emitter-Detector unit enable reliable measurement of NADPH fluorescence changes at a satisfactory signal/noise ratio and high time resolution.

9-AA and other fluorescent probes

The excitation spectrum of 9-amino-acridine (9-AA) fluorescence peaks around 400 nm, with shoulders around 380 and 365 nm. The emission peaks are located at 430 and 475 nm. Schuldiner *et al*. (1972) first applied the quenching of 9-AA fluorescence upon illumination of thylakoids for determination of the transthylakoid membrane ΔpH. They assumed that only the deprotonated 9-AA base (pK 10) is freely permeable across the membrane, so that the protonated form will be trapped within the thylakoid lumen upon internal acidification, where its fluorescence is quenched. While the physical mechanism of 9-AA fluorescence quenching has been controversially discussed, it has found widespread practical applications in bioenergetical and plant physiological studies with isolated thylakoids (e.g. Avron and Schreiber 1977) and intact chloroplasts (e.g. Tillberg *et al*. 1977; Hormann *et al*. 1994).

While in principle, fluorescent probes can be also applied for monitoring internal pH changes in spheroplasts or whole cells from different phototrophic organisms, the observed changes are more complex and more difficult to interpret. A comprehensive study of fluorescent probes for bioenergetic studies of whole cyanobacterial cells was presented by Teuber *et al*. (2001). Acridine orange and Acridine yellow proved to be the best ΔpH indicators for investigation of thylakoid and cytoplasmic membrane energization in *Synechocystis* PCC 6803. A special Acridine Orange/Yellow fluorescence module for the DUAL-PAM-100 has been available for some time. These dyes show excitation maxima around 430 and 460 nm, respectively, i.e. shifted to longer wavelengths with respect to 9-AA, and also the emission peaks are shifted into the green (peaks around 510 and 500 nm, respectively). While the emission is optimally detected by the photomultiplier sensor of the new NADPH/9-AA module, 365 nm excitation is suboptimal, with about 12% of maximal excitation in the case of Acridine orange and only about 5% in the case of Acridine yellow. Nevertheless, due to the high fluorescence yields and the superior sensitivity of the photomultiplier sensor, the new NADPH/9-AA is well suited for measuring Acridine orange and Acridine yellow changes.

The present communication concentrates on NADPH measurements and interpretation of the obtained data. Examples of applications of the new NADPH/9-AA module using 9-AA and various other fluorescent probes will be presented in a separate PAN article.

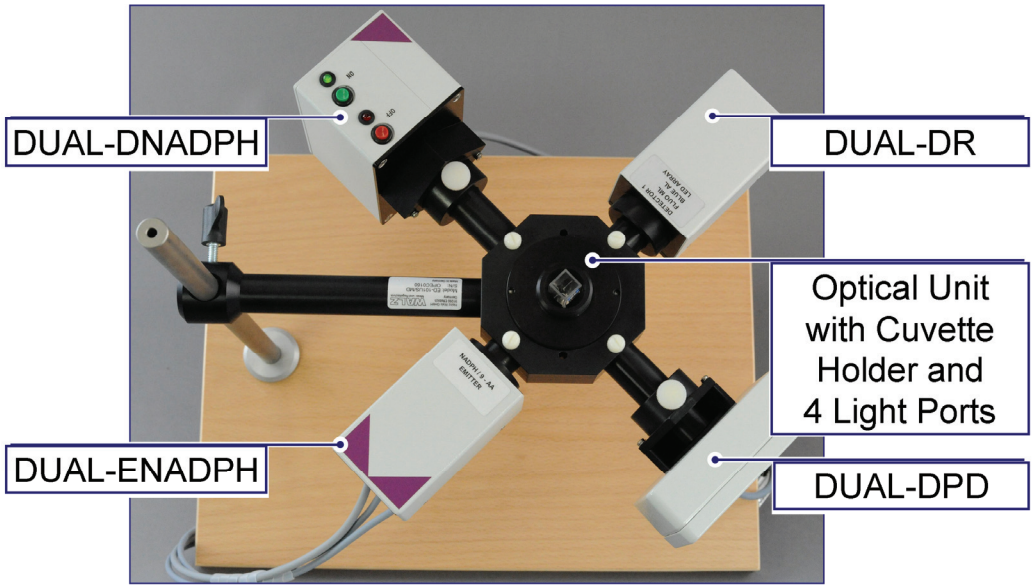

Fig. 1.

Emitter unit DUAL-ENADPH, photomultiplier detector (DUAL-DNADPH) of DUAL-DNADPH unit, separate photodiode detector DUAL-DPD and standard detector unit DUAL-DR mounted on the optical unit ED-101US/MD

Material and methods

Technical features of the NADPH/9-AA module

The NADPH/9-AA module consists of the emitter unit DUAL-ENADPH and the detector unit DUAL-DNADPH. The latter consists of a miniature photomultiplier with power supply which is approximately 1500x more sensitive than the photodiode detector employed by the standard DUAL-DR (or DUAL-DB) and almost 200-fold more sensitive than the optional, separate photodiode detector DUAL-DPD. The DUAL-ENADPH in outer appearance is equivalent to the standard emitter unit for simultaneous measurements of P700 and Chl fluorescence, DUAL-E.

For operation of the NADPH/9-AA module, the standard control unit DUAL-C and the optical unit ED-101US/MD for measurements with suspensions are required. Emitter and detector units are mounted at right angle with respect to each other. For simultaneous measurements of Chl fluorescence either the standard DUAL-DR or the optional, separate photodiode detector DUAL-DPD can be mounted on the optical port opposite to the photomultiplier. The DUAL-DPD is recommended for measurements with suspensions, as it is about 8 fold more sensitive. If, as normally the case, the standard DUAL-DR is available, this can be mounted at right angle to the DUAL-DPD and opposite to the DUAL-ENADPH, with only the LED Array cable being connected to the DUAL-C (see Fig. 1). In this way, the sample can be homogenously illuminated from opposite sides.

Emitter unit DUAL-ENADPH

The DUAL-ENADPH contains a UV-A (365 nm) Power LED providing pulse-modulated NADPH/9-AA fluorescence measuring light. A red LED (620 nm) is employed for pulse-modulated Chl fluorescence measuring light. A Chip-On-Board LED Array (635 nm) serves for continuous actinic illumination (max. 2000 µmol $m^{-2}s^{-1}$ PAR), saturating Single Turnover flashes and Multiple Turnover flashes (max. 20000 µmol·m^{-2}·s^{-1} PAR). A far-red LED (730 nm) provides light for preferential excitation of PS I. All optical filters are permanently mounted within the DUAL-ENADPH housing:

a. The UV-A excitation light is filtered by a short-pass filter with $\lambda<400$ nm
b. The red Chl fluorescence excitation light is filtered by a short-pass filter with $\lambda<645$ nm
c. The red actinic light is passing a long-pass filter with $\lambda>600$ nm to remove a small fraction of yellow-green emission of the red LEDs.

The various types of LED light feed into a 10x10x50 mm quartz rod, which serves for guiding the randomized light to the 10x10 mm cuvette containing the sample.

The DUAL-ENADPH is connected with 3 cables to the input sockets EMITTER, LED ARRAY and FLUO ML of the DUAL-C control unit.

Detector unit DUAL-DNADPH

The DUAL-DNADPH features a photomultiplier (DUAL-DNADPH) detector with automatic overload switch-off and manual On/Off buttons. The DUAL-DNADPH displays maximal sensitivity in the blue spectral range and is relatively insensitive in the red. The latter property is important for minimizing the effect of a spurious fraction of actinic light passing the filter set in front of the detector. The filter set transmits a broad blue-green band (420-580 nm). It consists of 3 filters which are optimized for

a. Eliminating pulse-modulated NADPH/9-AA excitation light
b. Absorbing the pulse-modulated Chl fluorescence
c. Absorbing the strong actinic light originating from the Chip-On-Board LED Array.

The DUAL-DNADPH features a filter box with cover and an adapter for mounting on the optical port featuring a 10x10x100 mm Perspex rod, which carries the fluorescence from sample to detector (see Fig. 1). The end of the Perspex rod should press gently against the filter. The DUAL-DNADPH is connected via the MULTIPLIER SUPPLY socket with its Power Supply and via the Detector 2 cable to the corresponding input socket of the DUAL-C control unit. The DUAL-DNADPH power supply offers 6 coarse and 12 fine sensitivity settings.

It is recommended to increase DUAL-DNADPH sensitivity until a signal between 3.5 to 4.5 V is reached. The software controlled Gain (under Settings/Mode/NADPH-Fluo) should be at setting 1 (Low), as signal amplification by the DUAL-DNADPH is better. The signal saturates at about 5 V. When the DUAL-DNADPH sensitivity is stepwise increased beyond signal saturation, first the signal noise disappears and then the signal may show large variations, jumping from positive to negative values. In order to rule out that the signal is saturated, the DUAL-DNADPH sensitivity should be stepwise decreased and ascertained that the signal amplitude is correspondingly decreased.

While the automatic overload switch-off protects the DUAL-DNADPH against damage by excess light, the performance of the DUAL-DNADPH is strongly affected by any non-modulated background light. In contrast to the standard photodiode detector, the DUAL-DNADPH noise increases with incident light intensity. Therefore, the cuvette compartment and the filter box should be always tightly closed. All optical ports that are not used have to be closed using the mirrored rods. This is also true for the bottom port, if the Miniature Magnetic Stirrer is not mounted. When the separate photodiode detector DUAL-DPD is mounted opposite to the DUAL-DNADPH, its filter box should be covered.

Separate photodiode detector DUAL-DPD

The DUAL-DPD is equipped with a 10x10mm photodiode matching the 10x10 Perspex light guide that leads the fluorescence from the 10x10mm cuvette to the detector. It features a filter holder, in which a 2mm RG665 filter (Schott) is mounted for Chl fluorescence measurements. While the DUAL-DPD employs the same photodiode as the standard DUAL-DR (and DUAL-DB) detector, it is about 8-fold more sensitive for two reasons:

a. The full 10x10 mm area is used, whereas in the DUAL-DR only a 6.5 mm diameter circular area is used (central hole in Chip-On-Board LED Array for actinic illumination).

b. The RG665 filter passes the short-wavelength Chl fluorescence peak, which in suspensions is about 3 fold higher than the far-red satellite peak. The DUAL-DR was optimized for simultaneous measurements of P700 and Chl fluorescence in leaves, where the short-wavelength peak is reabsorbed. Therefore, as the P700 signal is disturbed by strong short-wavelength red, the DUAL-DR is equipped with an RG9 filter (Schott) which opens at 715 nm and effectively absorbs the red actinic light.

Important points for optimal NADPH measurements

As outlined above (see section on background on NADPH fluorescence), NADPH fluorescence measurements in suspensions of isolated chloroplasts or photoautotrophic cells are impeded by a number of unavoidable, complicating factors. As a consequence, the signal is rather small and attention should be paid to optimize the signal/noise ratio. In this context, the following points have proven important:

a. Low fluorescent suspension media should be used to minimize the background signal, as the noise increases with overall signal amplitude.

b. Algae and cyanobacteria should be centrifuged and resuspended in fresh, low-fluorescent medium. In particular, any soil extract in the growth medium should be washed out, as it displays strong fluorescence upon 365 nm excitation.

c. Preferably young cells in the logarithmic growth phase should be used, as they not only show maximal physiological activity, but also a maximal ratio of NADPH/background fluorescence.

d. It is recommended to filter suspensions through a fine nylon mesh to remove particulate matter (dust particles, microscopically small fibers and debris), which not only increase the background signal, but also can cause large disturbances upon settling and when samples are stirred.

e. For measuring the dark-baseline, the time-integrated intensity of the measuring light (ML) has to be very low, in order to avoid NADPH accumulation before onset of actinic illumination (AL). On the other hand maximal ML intensity (setting 20) is advantageous with respect to a high signal/noise. These two conflicting aspects can be reconciled with each other by appropriate choice of ML frequencies in the absence and presence of AL. Maximal ML intensity setting 20 and frequency settings 200 and 5000 are recommended for MF Low and MF High, respectively. When Auto MF High is active, frequency automatically switches from MF Low to MF High upon onset of AL.

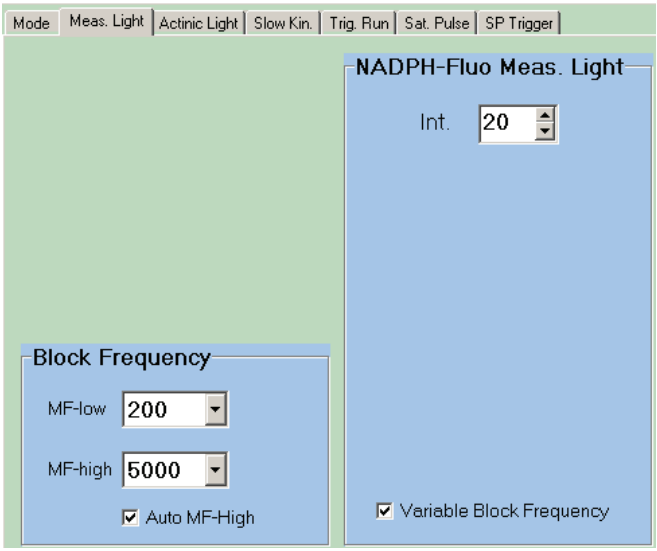

Fig. 2. The NADPH measuring light window permits adjustments of frequency and intensity off UV-A excitation.

Signal/noise performance and signal stability

Potential sources of signal noise and disturbances are the instrument (i.e. electronics, including LED emitter and photomultiplier detector) and the sample. In practice, often the sample noise is dominating. The noise originating from the instrument can be judged by measurements with a stable fluorescent standard. Fig. 3 shows a Slow Kinetics recording of 365 nm excited fluorescence of Lumogen Blue dissolved in ethanol at an acquisition rate of 1 millisecond/point. Measuring light frequency (MF) is switched from MF Low = 200 Hz to MF High = 5000 Hz and back. The same recording is displayed at 3 different settings of *Average Points* (on Slow Kinetics screen).

Figure 3 shows that the relative amplitude of the noise is substantially decreased with increasing MF and number of averaged data points. The MF increase from 200 to 5000 Hz results in a five-fold decrease of noise. With increase of the number of averaged points from 16 to 256, the noise is decreased by a factor of 8. While the MF settings, just like the analogue *Damping* (under Settings/Mode) have to be defined before a measurement, the number of points to be averaged can be chosen after the recording.

The recording presented in Fig. 3 indicates that the instrument related noise is mostly “white”, i.e. random, so that it can be minimized by point averaging, depending

on the required time resolution. At maximal Slow Kinetics acquisition rate of 1 millisecond/point even with 256 point averages the time resolution of about 4 points/second is sufficient for many applications. In applications where a higher time resolution is essential, the noise can be further decreased by curve averaging. In the given example, the noise apparent at MF High = 5000 Hz that persists with 256 point averages, amounts to about 0.1% of the total signal.

On close look a small signal rise upon switching from MF Low to MF High is apparent (see 5 fold sensitivity trace in Fig. 3). This signal rise can be explained by an "induction effect" of the UV-A LED. It is more pronounced at MF High = 10000 Hz (not shown). It also is enhanced when the UV-A LED has not been switched on for a longer period of time (e.g. over night). While this artefact is of no concern when light-induced changes are in the order of 5-20%, it may disturb measurements with samples under unfavorable conditions, when changes in the order of 1% are analyzed. In this case, it is recommended to switch on the measuring light (N ML) at MF High = 5000 Hz for about 10 min before starting serious experiments.

The sample-related noise is least with chloroplasts suspensions, which almost perform like the Lumogen fluorescence standard, provided they are filtered through a fine nylon mesh to avoid disturbance by moving tissue debris. Fig. 4 shows a typical experiment with continuously stirred hypotonically broken spinach chloroplasts in the presence of 2 µM NADP at 16 point averages.

First 0.4 µM NADPH is added for signal calibration at MF Low (200 Hz). Then actinic light is switched on with Auto MF High switching to high measuring light frequency (5000 Hz). NADP reduction is first linear and then levels off when NADP becomes exhausted. The relative noise amplitude is very similar to that observed with the Lumogen standard (Fig. 3) at 16 point averages. Notably, there is no significant increase of noise caused by the stirring.

In this experiment the Miniature Magnetic Stirrer US-MS with a 6 x 1.5 mm magnetic stir bar (Starna) was used at maximal stirring rate. The design of the Optical Unit ED-101US/MD is such that the bottom of the quartz cuvette is directly on top of the stirrer and the stir bar 2 mm below the lower edge of the Perspex rod guiding the fluorescence from the sample to the detector. Therefore, the detector does not "see" the stir bar and if there is any stirring noise, this is likely to originate from moving particulate matter. This can be readily checked by visual inspection with actinic light at moderate intensity switched on, by viewing via an opened side port. Even a tiny piece of cellulose fiber, barely visible by bare eye, can cause a more than 10 fold increase in sample noise.

Addition of a small NADPH aliquot can serve for calibrating the light-induced NADPH changes and also for estimating the detection limit of the NADPH/9-AA module for NADPH. In the example of Fig. 4, the noise at MF High is about 1/25 of the change corresponding to 0.4 µM NADPH. Hence, a detection limit of about 50 nM NADPH is estimated. This can be further lowered by signal averaging.

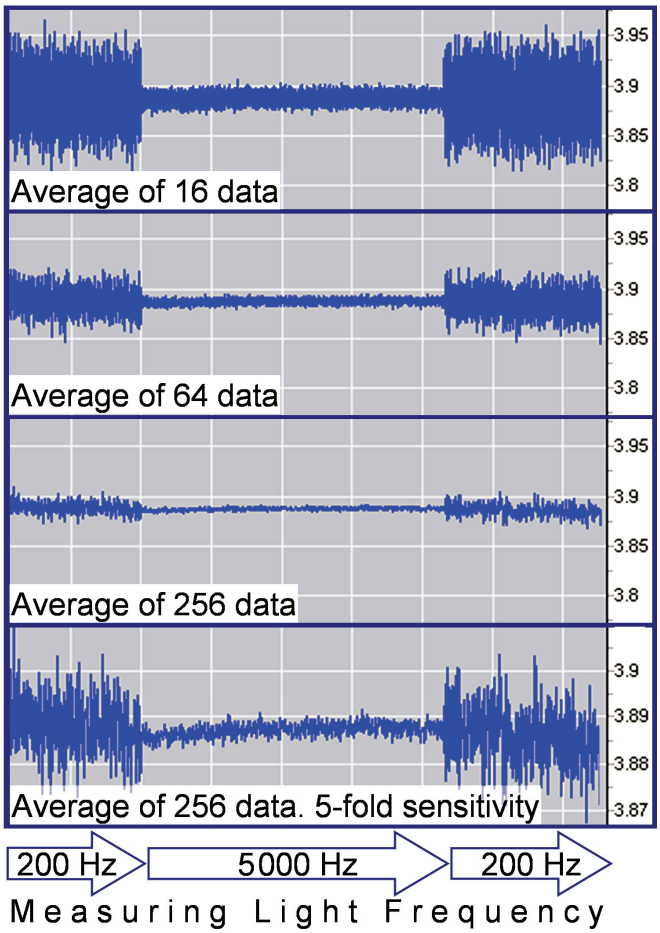

Fig. 3. Assessment of instrument related noise by Slow Kinetics recording of fluorescence signal of Lumogen Blue at Acquisition Rate of 1 millisecond/point, MF Low = 200 Hz and MF High = 5000 Hz. Display of the same recording at 3 different indicated settings of *Average Points*. The trace with 256 *Average Points* is also presented at 5 fold sensitivity. Time units, 1 min.

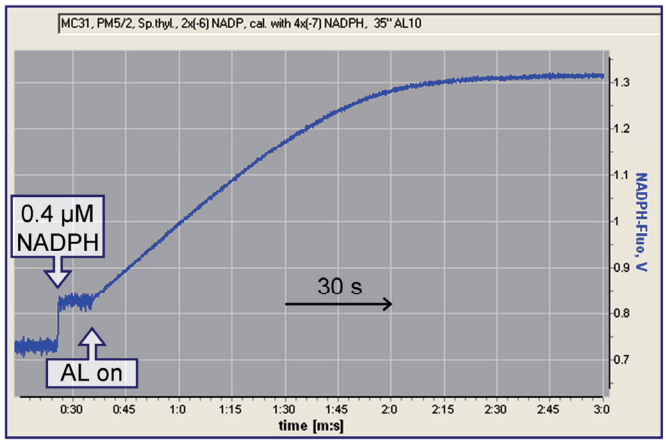

Fig. 4. Demonstration of signal/noise performance in Slow Kinetics recording of continuously stirred broken spinach chloroplasts in the presence of 2 µM NADP. Arrows indicate (1) addition of 0.4 µM NADPH and (2) start of actinic illumination of 600 µmol·m^{-2}·s^{-1}. The Auto MF High function switched the measuring light frequency from 200 to 5000 Hz. Display with 16 *Average Points*.

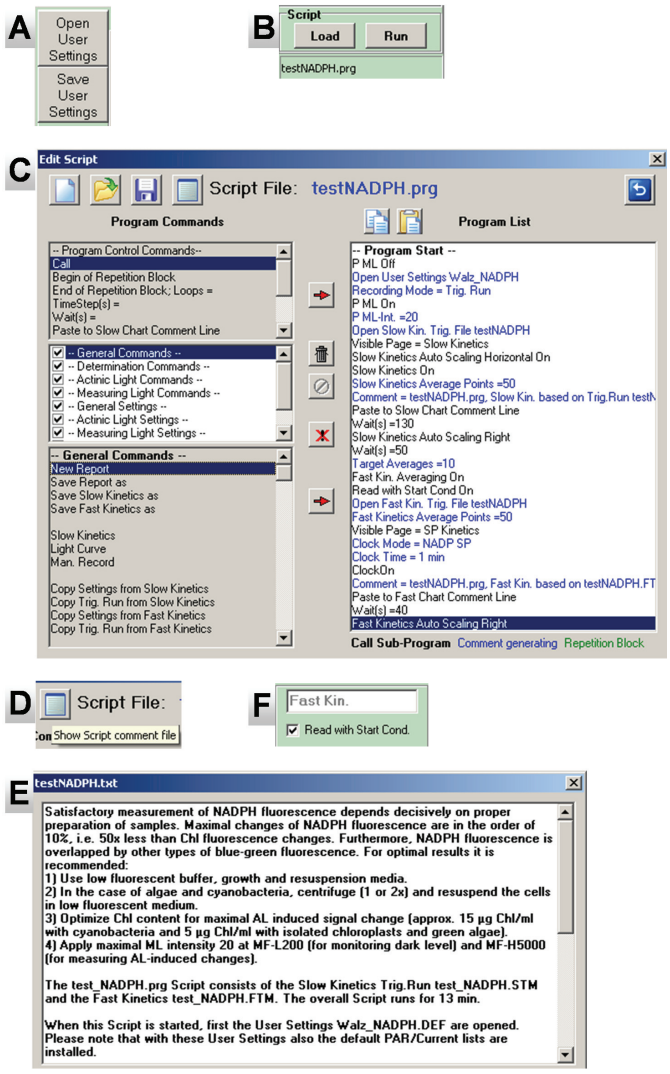

Fig. 5. Elements of graphical user interface to control instrument settings and script files.

Special User Settings and files for NADPH measurements

The same Dual-PAM software is used for operation of the NADPH/9-AA module as for standard Chl fluorescence and P700 measurements. Hence, users familiar with the standard applications should not have much problems operating the NADPH/9-AA module. In the following some hints for making optimal use of this software in conjunction with the NADPH/9-AA module are given.

Before starting NADPH measurements, it is recommended to open the settings file Walz_NADPH.def using the "Open User Settings" command (Fig. 5A). In this way, it is made sure that appropriate settings are effective, that differ from default settings for standard Chl fluorescence experiments and have proven optimal for NADPH measurements (e.g. ML intensity 20).

The Script testNADPH.prg was programmed to demonstrate two useful Trigger files, the Slow Kinetics testNADPH.STM and the Fast Kinetics testNADPH.FTM. The Script file is opened via the *Load* button and started via *Run* (Fig. 5B).

The Program list (Fig. 5C) shows the consecutive commands of the Script file. First the essential settings are installed. Then a Triggered Run with Slow Kinetics involving a 100 s actinic illumination is measured. Finally 10 Fast Kinetics recordings involving a 15 s actinic illumination are averaged. The user may readily modify the Script program as well as User settings and Trigger files and save them under new names.

The Script Comment File associated with the current script file can be opened using the "Open Comment" button (Fig. 5D). Script Comment files (Fig. 5E) can be edited. When the Triggered Run testNADPH.STM is opened, automatically also the appropriate Acquisition parameters (256000 Acquisition Points, 1 ms/p Acquisition Rate under Settings/Slow Kin.) are installed. Appropriate settings are also installed upon opening the Fast Trigger file testNADP.FTM, if Read with Start Cond. (Fig. 5F) is enabled on the Fast Trigger window.

Averaging of recordings and repetition clock

When the signal/noise ratio of single recordings is not satisfactory, it can be improved by averaging of a number of recordings. Manual and automatic averaging routines are provided. Manual Averaging involves selection of the corresponding files from a drop-down list (Fig. 6A), which is opened by clicking the "+" icon (on Slow and Fast Kinetics windows).

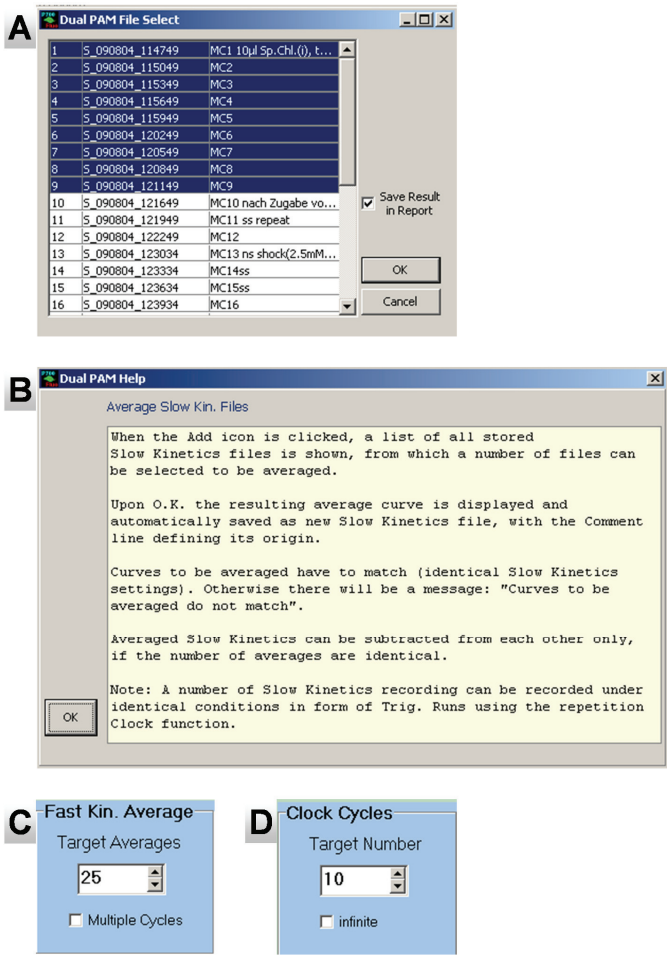

Fig. 6. Elements of graphical user interface to control averaging of kinetics.

In this context, the user is encouraged to make use of the Help-texts (see Fig. 6B) accessible via the F1-command, when the function element in question is selected by the cursor. In view of the complexity of the Dual-PAM software, these texts can be quite helpful to make optimal use of the system.

Fast Kinetics can be averaged either manually (by selection from a drop-down list, as in the case of Slow Kinetics) or automatically, after enabling *Averaging* on the Fast Kinetics window. The desired number of averages is defined under Settings/Fast Acqui./*Target averages* (Fig. 6C).

The Clock (see Fig. 6D) can be applied for averaging repetitive measurements with defined time intervals in between. In the case of Fast Kinetics, the Clock just has to be started. It stops when the Target averages are reached. While Slow Kinetics cannot be automatically averaged, the Clock still is useful for triggering consecutive recordings with defined time intervals. The desired number of Clock cycles can be set under Settings/Slow Kin./Clock Cycles/*Target Number*.

Results and discussion

Fig. 7A shows typical dark-light-dark induction transients of NADPH fluorescence measured with a suspension of dark-adapted intact spinach chloroplasts using the Triggered Run testNADPH.STM. Interestingly, the dark-adapted signal level is distinctly higher than the dark level following the 100 s illumination period, suggesting that about 35 % of the NADP pool is reduced after dark-adaptation. This observation is in agreement with measurements of Takahama *et al.* (1981), who determined the amount of NADP and NADPH by enzymatic cycling and found that between 40 and 60 % of the chloroplast NADP was reduced in the dark.

The initial rise of light-induced NADPH fluorescence can be resolved, when a number of Fast Kinetics are averaged using the automatic Averaging and Clock functions. Fig. 7B shows 10 averages based on the Fast Trigger file testNADPH.FTM. While the complete recording runs for 32 s, only the first 2 s with the initial rise are displayed. The initial rise kinetics reveals two phases of NADP reduction. On closer inspection at horizontally zoomed time scale a distinct lag phase of about 10 ms is apparent (not shown). Important kinetic information is also obtained following AL off, reflecting NADPH re-oxidation via various alternative reactions in the dark (related to Calvin-Benson cycle, cyclic PS I, detoxification of reactive oxygen species, nitrite reduction etc.), detailed discussion of which would be out of scope of this application note.

In contrast to Chl fluorescence, the initial rise of NADPH fluorescence does not directly reflect charge separation at PS I, as NADP is not the primary acceptor of P700. The thermal electron transfer steps between the primary PS I acceptor A_0 and NADP should be reflected by the kinetics of the signal change induced by a saturating single turnover flash. As demonstrated in Fig. 8, the signal rise induced by a saturating 40 µs flash (ST40µs) can indeed be evaluated, when 100 Fast Kinetics recordings are averaged. The displayed curve is the difference of the kinetics measured with ST40µs triggered at time 0 and without ST40µs, in order to correct for the fluorescence rise induced by the measuring light at high MF. As was already noticed by Cerovic *et al.* (1993), NADPH accumulates at very low light intensity. Therefore, the measuring light was switched on only briefly before start of the recording using the *Auto ML on* function.

A single 40 µs flash induces approximately 1/6 of the maximal signal change (Fig. 8). As already suggested by the data in Fig. 7, there is a lag phase of about 10 ms before the signal starts rising and the rise consists of two equal size phases, with half-times of about 10 and 60 ms. It remains to be clarified, whether the two phases possibly reflect two types of NADP pools or two pathways of NADP reduction.

In presence of 1 µM DCMU the light-induced fluorescence rise consists of two distinct phases that are sepa-

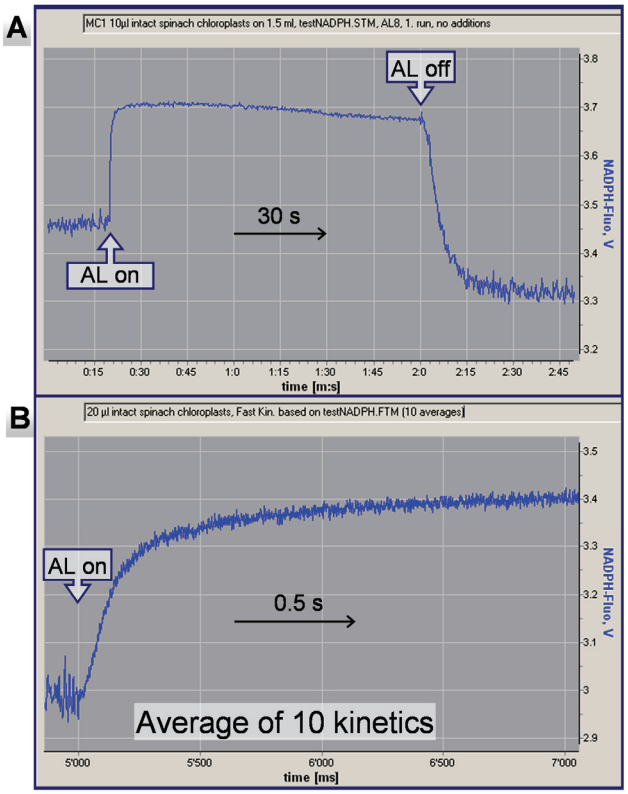

Fig. 7. A: Slow Kinetics recording (testNADPH.STM) of dark-light-dark induction transients of dark-adapted intact spinach chloroplasts. Light intensity, actinic light intensity setting AL=8, 380 µmol·m^{-2}·s^{-1}. Display with 256 *Average Points*. **B:** Fast Kinetics recording of light-induced increase of NADPH fluorescence in intact spinach chloroplasts. At 5000 ms light-on (actinic light intensity setting AL=8, 380 µmol·m^{-2}·s^{-1}) and MF switched from Low 200 to High 5000. 10 averages with 1 min repetition intervals. Acquisition rate, 1 ms/point. Display with 1 *Average Points*.

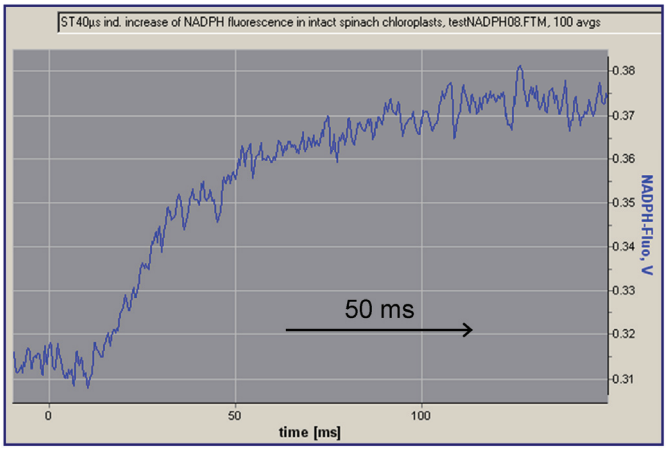

Fig. 8. Fluorescence rise induced by a 40 µs saturating flash in intact spinach chloroplasts. The trace corresponds to the average of 100 curves observed in the presence of a flash minus the 100 curves average in the absence of a flash. The flash was triggered at time 0 and *Auto ML on* was enabled. Acquisition rate 5 µs/point. Display with 64 *Average Points*.

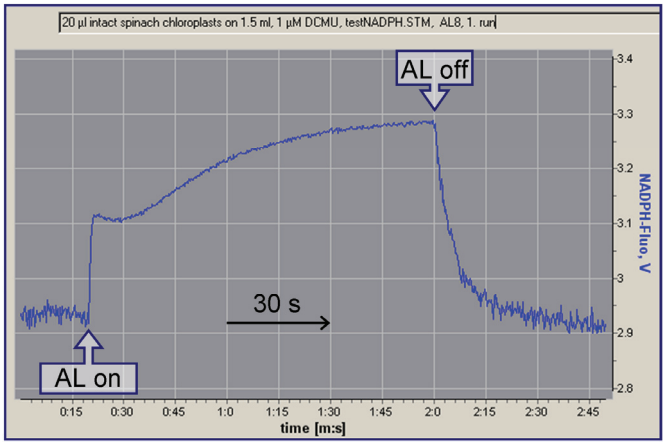

Fig. 9. Slow Kinetics recording (testNADPH.STM) of dark-light-dark induction transients of dark-adapted intact spinach chloroplasts in the presence of 1 µM DCMU. Light intensity, 380 µmol·m^{-2}·s^{-1}. Display with 256 *Average Points*.

rated by a small dip phase. Closer inspection of the fast phase after horizontal zoom reveals a half-rise time of 140 ms (not shown in the figures), which is very similar to the half-rise time in the absence of DCMU. The slow phase, which starts with 10 s delay, is characterized by a half-rise time of 23 s. The latter is accelerated by preillumination (not shown).

Dark-light-dark induction transients of NADPH in *Chlorella vulgaris*

Typical dark-light-dark induction transient of *Chlorella vulgaris* at 3 different actinic light intensities are shown in Fig. 10. While the curve at an actinic light intensity of 380 µmol·m^{-2}·s^{-1} was recorded after 5 min dark-adaptation, the consecutively measured curves (70 and 20 µmol·m^{-2}·s^{-1}) were recorded after 90 s dark time. As already observed with isolated intact chloroplasts (Fig. 7A), after 5 min dark-adaptation a substantial fraction of NADP (38 %) is already reduced in the dark. After 90 s dark time only about 15 % of the total NADP pool is reduced.

The light-induced changes in *Chlorella* are more complex than those observed in isolated chloroplasts. The changes at 380 µmol·m^{-2}·s^{-1} resemble the changes in isolated chloroplasts in the presence of 1 µM DCMU (Fig. 9).They reveal a dynamic interplay of reduction and oxidation reactions. At actinic light intensities of 20 and 70 µmol·m^{-2}·s^{-1}, the initial rise is followed by a pronounced dip phase, before a second rise phase sets in. At 380 µmol·m^{-2}·s^{-1}, and at 70 µmol·m^{-2}·s^{-1}, after about 40 s illumination, the NADPH fluorescence yield starts declining again. This decline is likely to reflect NADPH consumption by CO_2 fixation. Following activation of the Calvin-Benson cycle by preillumination, the decline is enhanced and shifted to shorter times (see below).

While on first sight, the NADPH fluorescence induction kinetics in *Chlorella* may resemble the O-I-D-P-S transients of Chl fluorescence (Kautsky effect), the early transients of the latter are distinctly faster. Simultaneous measurements of NADPH and Chl fluorescence are presented in Fig. 11.

Fig. 11 shows simultaneous recordings of dark-light-dark induced changes of NADPH and Chl fluorescence in *Chlorella vulgaris*. Calvin-Benson cycle enzymes were light-activated due to repetitive illumination triggered with 4 min clock intervals. The displayed data are the average of 4 recordings. Under the given conditions, the NADPH induction kinetics are dominated by a peak about 25 s after onset of illumination and a pronounced NADPH reoxidation phase upon light-off. The NADPH peak coincides with a secondary peak of Chl fluores-

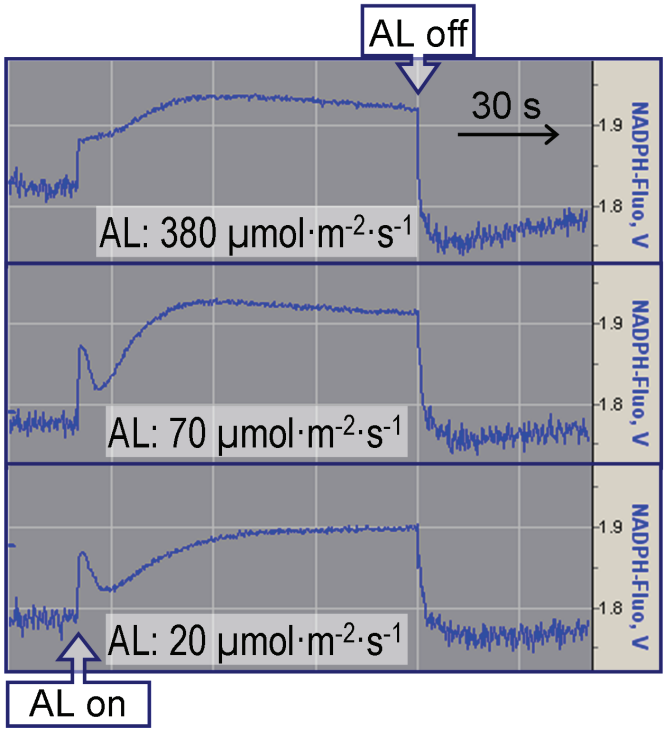

Fig. 10. Slow Kinetics recording (testNADPH.STM) of dark-light-dark induction transients of *Chlorella vulgaris* at three actinic light intensities (AL). Display with 256 *Average Points*.

cence, presumably corresponding to the M1-peak described in the literature (see e.g. Renger and Schreiber, 1986). For resolving the O-I-P transients, in Fig. 11B the early parts of the curves are displayed at zoomed scales.

While the O-I rise of Chl fluorescence reflects the reactions at the acceptor side of PS II, the I-P rise has been interpreted to reflect transient exhaustion of electron acceptors at the PS I acceptor side and the P-S decline occurs when this limitation is overcome. The presented data are in agreement with this interpretation and allow some additional insights. Most of the rapid phase of NADP reduction, which is completed 300 ms after AL-on, occurs during the 200 ms of constant Chl fluorescence yield at the I-level. The dip in NADPH fluorescence sets in before the Chl fluorescence peak, P, is reached, which at the given low light intensity is much lower than the maximal fluorescence yield, Fm. Hence, the reoxidation of NADPH expressed in this dip, appears to be responsible for P being photochemically quenched with respect to Fm. The question arises, by what mechanism NADPH is reoxidized already 300 ms following onset of illumination. The data in Fig. 11C suggest that molecular oxygen is involved.

Fig. 11C can be directly compared with Fig. 11A, as the same sample under identical conditions was used, except for the removal of molecular oxygen. It is apparent that the dip-phase in NADPH fluorescence is eliminated. When longer periods of anoxia are applied, NADP becomes almost completely reduced in the dark and Chl fluorescence yield increases to the Fm level (data not shown in the figures; see Schreiber and Vidaver 1974, 1975).

Dark-light-dark induction transients of NADPH in cyanobacteria suspensions

Dark-light-dark induction transients of NADPH in *Synechocystis* PCC 6803 and of its ndh-B defective mutant M55 were already measured by Mi *et al.* (2000) using a modified PAM fluorometer. In this work, the cells were illuminated repetitively (10 s light/40 s dark intervals) and the responses of 10 dark-light-dark curves were averaged. Analysis of the observed transients in the presence of artificial electron acceptors and inhibitors led to tentative interpretations of the various induction transients.

Measuring NADPH fluorescence in cyanobacteria can be complicated by a strong background signal, which not only leads to an increase of noise, but also to substantial signal drift. Most of this background signal is due to a fluorescent substance excreted by the cyanobacteria during growth. This can be demonstrated by comparing the responses of the same cells in the original growth suspension and after centrifugation/resuspension in the same volume of fresh growth medium.

As can be seen in Fig. 12, the signal/noise ratio of resuspended *Synechococcus* PCC 7942 cells is about 10 times higher than that of the original suspension. Furthermore,

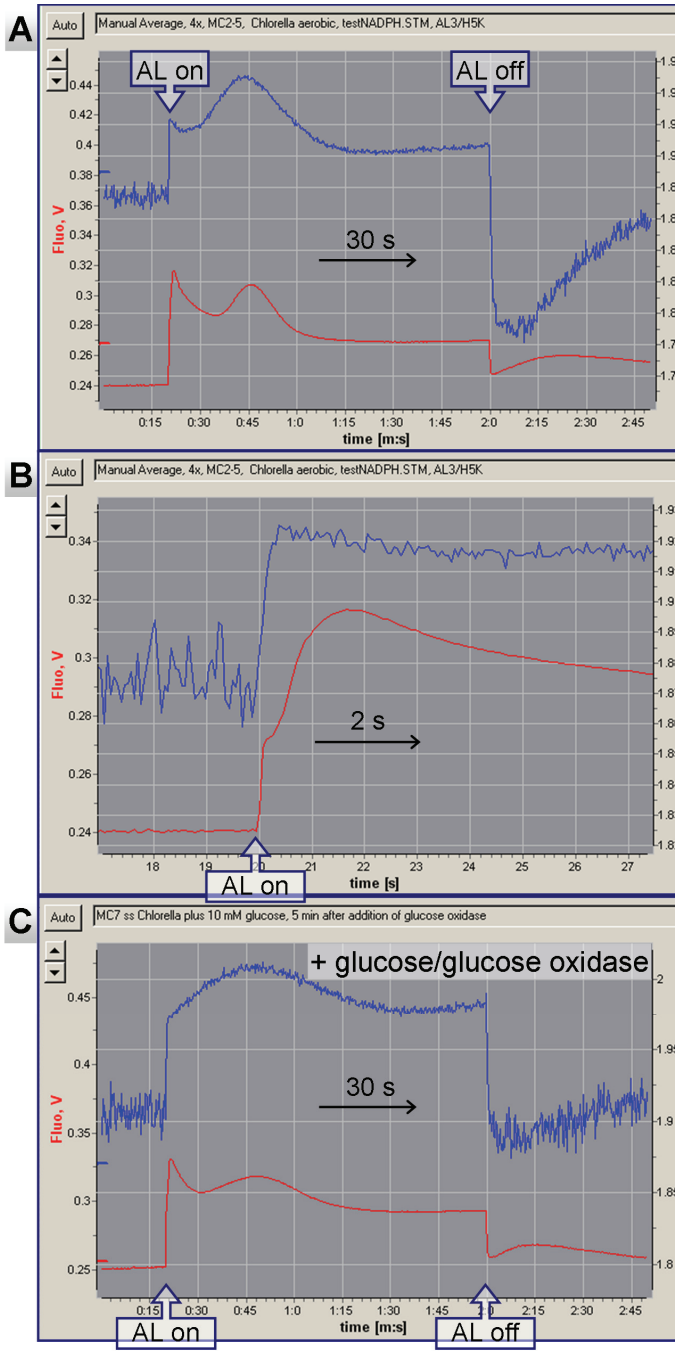

Fig. 11.

A: Simultaneously measured Slow Kinetics (testNADPH.STM) of NADPH and Chl fluorescence of *Chlorella vulgaris*. Fluo ML intensity, setting 5. Actinic light intensity, AL3, 70 µmol quanta/m²s. Average of 4 recordings measured with 4 min Clock intervals. Display with 256 *Average Points*.

B: Identical recordings as in panel A with the early part being zoomed for resolving O-I-P transients of Chl fluorescence rise. Display with 64 *Average Points*.

C: *Chlorella vulgaris* 5 min after addition of glucose/glucose oxidase for removal of molecular oxygen. Otherwise identical conditions and same sample as in panel A.

the positive signal drift observed in the original suspension, is disappeared after resuspension. Analysis of the background signal reveals that it is stimulated by sample illumination, particularly under physiological stress. Once an increase of this signal is induced by light, the

signal continues increasing for some time, before a slow decline sets in. The emission spectrum of the background signal extends over the whole blue-green region, just like that of NADPH, with the peak being shifted by at least 50 nm towards longer wavelengths. Hence, a flavine compound might be involved. While this background signal can be very disturbing with measurements of NADPH fluorescence, it may turn out to be a valuable indicator for a so far unknown mechanism of photoprotection in cyanobacteria. Further discussion of this aspect would be out of scope of this report.

The light-induced NADPH fluorescence changes of *Synechococcus* PCC 7942 depicted in Fig. 12 are characterized by a single rise phase and a very pronounced post-illumination peak. At lower actinic intensity (70 µmol·m^{-2}·s^{-1}) two rise phases and a small decline are apparent while the post-illumination peak is disappeared (not shown in the figures).

Simultaneously measured NADPH and Chl fluorescence changes of *Synechocystis PCC 6803* are shown in Fig. 13. For obtaining the depicted kind of dynamic responses, preillumination of the sample is essential in order to activate the reactions at the acceptor side of PS I. Distinct parallel and anti-parallel phases of NADPH and Chl fluorescence are apparent. The NADPH peak about 25 s after light-off is paralleled by a second post-illumination peak in Chl fluorescence. The first post-illumination Chl fluorescence peak is already observed 2 s after light-off, with the rise phase corresponding to the decay of NADPH. This first post-illumination peak of Chl fluorescence may correspond to the peak described by Mano *et al.* (1995) in intact chloroplasts, which was interpreted to reflect light activated electron flow from NADPH to plastoquinone involving ferredoxin and the FNR. The origin of the newly observed second post-illumination peak remains to be elucidated.

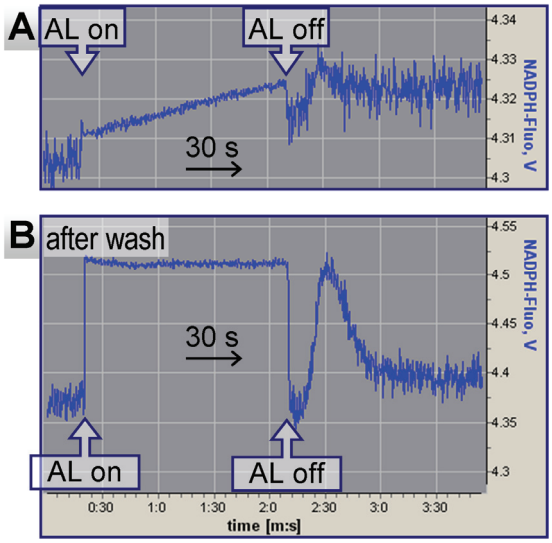

Fig. 12. Comparison of dark-light-dark responses of original *Synechococcus* PCC 7942 suspension (**A**) with the responses of the same cells after centrifugation and resuspension in the same volume of fresh medium (**B**). Actinic intensity, 380 µmol µmol·m^{-2}·s^{-1}. Display with 256 *Average Points*.

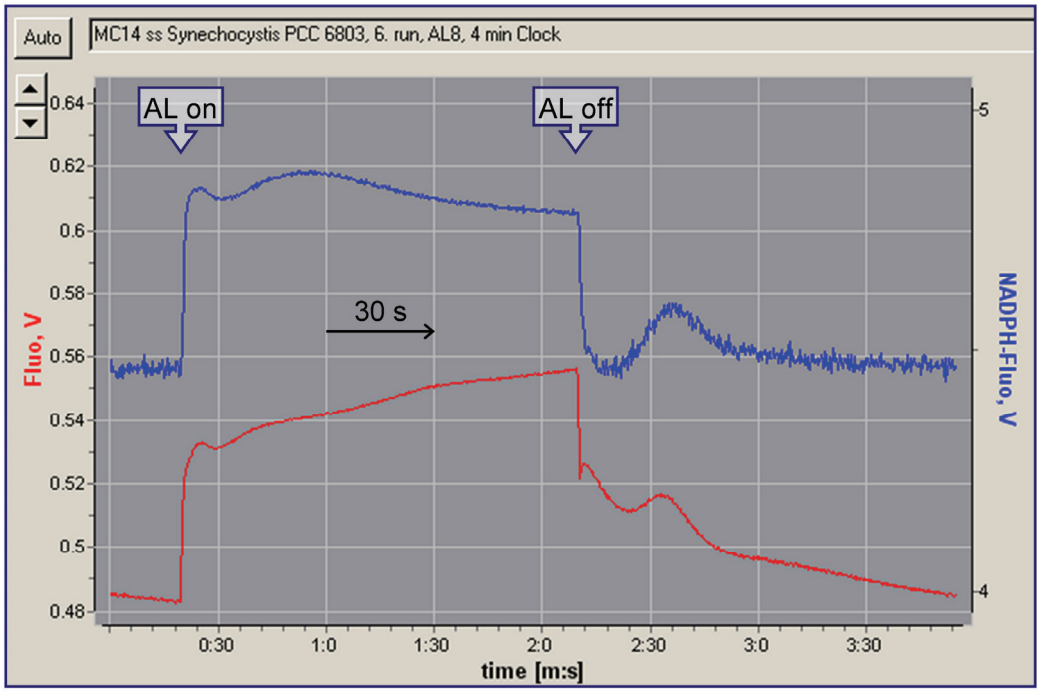

Fig. 13. Simultaneously measured dark-light-dark induction kinetics of NADPH and Chl fluorescence in Synechocystis PCC 6803. Cells centrifuged and resuspended in fresh medium. Preillumination by 110 s light/125 s dark cycles. Single recording. Actinic light intensity, 380 µmol·m^{-2}·s^{-1}. Display with 256 *Average Points*.

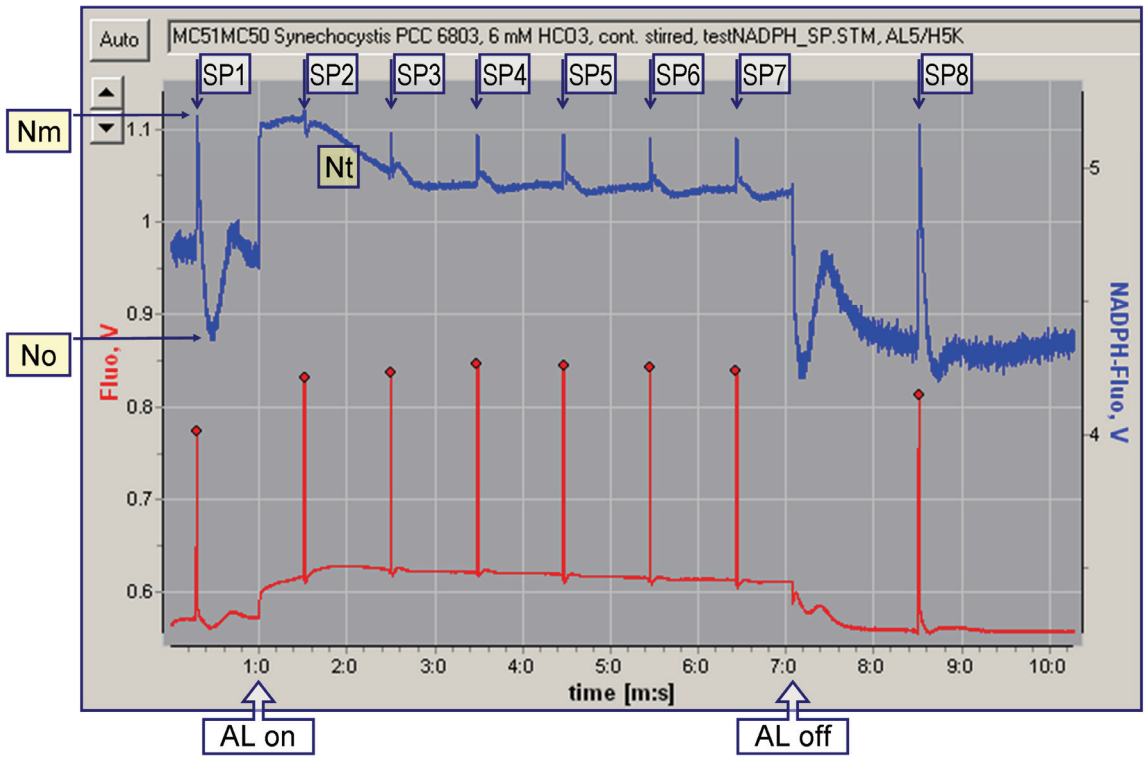

Fig. 14. Simultaneous measurements of dark-light-dark induction kinetics of NADPH and Chl fluorescence in *Synechocystis* PCC 6803 with application of Saturation Pulses (SP). Cells centrifuged, resuspended in fresh medium and continuously stirred. 5 min dark period between 5 min preillumination at 380 µmol·m^{-2}·s^{-1}, and start of recording. Actinic light intensity 180 µmol·m^{-2}·s^{-1}. SP intensity, 4000 µmol·m^{-2}·s^{-1}, SP duration, 800 ms. Display with 64 *Average Points*.

The Saturation Pulse (SP) method (Schreiber *et al.* 1986) has proven very useful for interpreting the complex phenomenology of light-induced Chl fluorescence changes and for obtaining quantitative information on the relative rate of electron transport in the steady state. The rationale of this method relies on the assumption that PS II reaction centers can be completely closed during a short SP, so that maximal fluorescence yield can be measured. In this way, changes in the maximal fluorescence yield due to non-photochemical quenching can be measured and redox-related changes (photochemical quenching) can be differentiated from energy or state related changes (non-photochemical quenching). A modified SP method was introduced for assessment of PS I quantum yield and P700 redox state (Klughammer and Schreiber 2008).

The question arises, whether the application of SP can also help analyzing NADPH fluorescence changes. Assuming linearity between NADPH concentration and NADPH fluorescence, the signal levels No and Nm for fully oxidized and fully reduced NADP, respectively, can be defined. Hence, if No and Nm were known, the current signal Nt would give information on the relative extent of NADP reduction in the given state of illumination, with the fraction of reduced NADP equaling (Nm-Nt)/(Nm-No).

In Fig. 14 simultaneous measurements of NADPH and Chl fluorescence in *Synechocystis* PCC 6803 with SP analysis are presented. It is apparent that under the given, favorable conditions SP analysis may provide additional information not only for interpreting Chl fluorescence, but NADPH changes as well. In this context, favorable conditions mean:

a. low background signal (centrifugation, resuspension in low fluorescence medium, filtering through narrow nylon mesh to remove particulate matter)

b. continuous stirring (to avoid settling and to stabilize oxygen content)

c. use of light-activated sample with high CO_2 fixation capacity and of relatively low actinic intensity, as otherwise NADP would remain mostly reduced, irrespectively of the rate of CO_2 fixation.

In the recording of Fig. 14, the change of the NADPH signal amounts to almost 20% of the overall signal, which is relatively high for measurements with cyanobacteria. Application of Saturation Pulses (SP-width 800 ms) causes spikes of NADPH fluorescence in the Slow Kinetics display. On the SP Kinetics window these spikes can be resolved into 200 ms rise and 600 ms plateau phases (see Fig. 15A-C). The signal quality allows to determine the Nm level with high accuracy. As already shown for intact chloroplasts and *Chlorella* (Figs. 7, 10 and 11), also in *Synechocystis* a substantial fraction of NADP can be reduced after dark-adaptation.

Under the given conditions, after full NADP reduction during the SP, there is a rapid transient reoxidation distinctly below the dark level (Fig. 14, for detail see Fig. 16). Upon onset of continuous actinic illumination, NADP first becomes almost completely reduced, as an

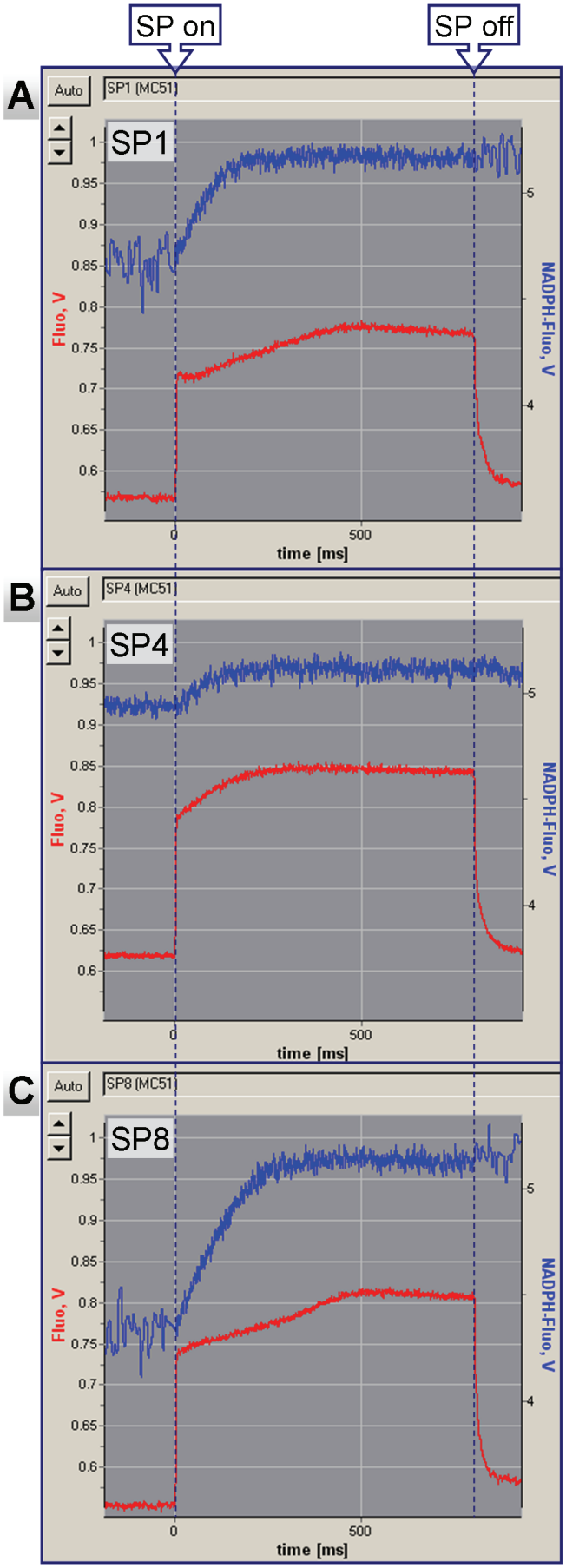

Fig. 15. Simultaneously measured kinetics of SP induced changes of NADPH and Chl fluorescence, as displayed on the SP Kinetics window for SP1, SP4 and SP 8 of the Slow Kinetics recording displayed in Fig. 14. Display with 4 *Average Points*.

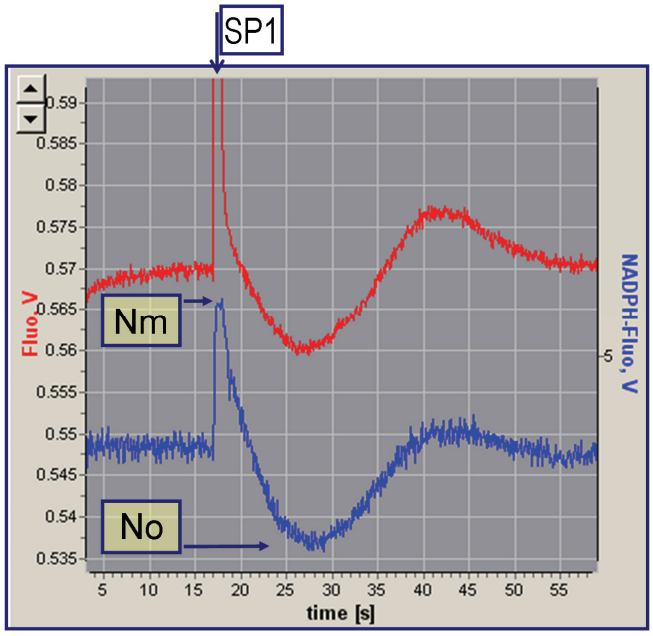

Fig. 16. Early part of recording depicted in Fig. 14 displayed at expanded scales.

SP causes a negligibly small signal increase followed by a transient dip. When the signal slowly decreases ($t_{1/2} \approx 1$ min), the SP induced spikes return, thus confirming that the signal decrease is indeed due NADPH reoxidation.

The last SP, which is applied 90 s after light-off, induces almost the same Nm as the first SP applied before actinic illumination, which shows that signal drift is negligibly small. When higher actinic intensity is applied, the current signal, Nt, and the maximal signal induced by SP, Nm, are identical, both declining during the 6 min illumination period and fully recovering again during a consequent 5 min dark period (data not shown). If it is assumed that NADPH remains fully reduced, there seems to be some mechanism of light-dependent, reversible NADPH fluorescence quenching. SP analysis can help to distinguish between this type of quenching, which is not suppressed by an SP, and the apparent "quenching" by NADP, which is suppressed by an SP.

The simultaneously measured changes of Chl fluorescence depicted in Fig. 14 are relatively small, as the applied actinic intensity is low and does not induce a major limitation at the PS II acceptor side. The Fm' increases upon actinic illumination, reflecting a state 2-state 1 shift (Schreiber *et al.* 1995). The Chl fluorescence SP kinetics reveals two major rise components (photochemical and thermal). As shown in Fig. 15, the simultaneously measured rise in NADPH fluorescence appears to parallel the first phase (I_1-I_2) of the thermal component.

Conclusions and outlook

The presented examples of applications demonstrate that the new NADPH/9-AA module allows to measure NADPH fluorescence changes with high sensitivity and time resolution in suspensions of isolated chloroplasts, green algae and cyanobacteria. With proper use of the extensive user software even small changes in the order of 1-2 % can be reliably analyzed. In particular, for the sake of NADPH measurements, the software has been extended to allow averaging of Slow Kinetics recordings.

A decisive prerequisite for measuring low noise NADPH fluorescence signals is the absence of a major background signal due to UV-A excited fluorescence of the suspension medium. As algae and cyanobacteria excrete strongly fluorescing substances into the growth medium, it is important that cells are centrifuged, washed and resuspended before measurements.

The NADPH fluorescence signal carries a wealth of information that hitherto has not been generally accessible due to lack of appropriate instrumentation. This information primarily relates to the redox state at the PS I acceptor side, the relative reduction of the NADP pool and the activation of various pathways of NADP-reduction/NADPH-oxidation in the light and in the dark. In this application note only a few examples are presented, which spotlight some of the typical information. At the present state of knowledge, all interpretations of the observed changes should be considered tentative. Extensive systematic research using this new tool will be required to establish a solid building of interpretations, similarly as in the case of Chl fluorescence changes. In this context, it is very important that Chl fluorescence can be readily measured simultaneously with NADPH fluorescence, so that the information carried by the Chl fluorescence changes can be used to interpret NADPH fluorescence changes.

References

Avron M, Schreiber U (1977) Proton gradients as possible intermediary energy transducers during ATP driven reverse electron flow in chloroplasts. FEBS Lett 77: 1-6

Cerovic ZG, Bergher M, Goulas Y, Tosti S, Moya I (1993) Simultaneous measurement of changes in red and blue fluorescence in illuminated isolated chloroplasts and leaf pieces: The contribution of NADPH to the blue signal. Photosynth Res 36: 193-204

Duysens LNM, Amesz J (1957) Fluorescence spectrophotometry of reduced phosphopyridine nucleotide in intact cells in the near-ultraviolet and visible region. Biochim Biophys Acta 24: 19-26

Hormann H, Neubauer C, Schreiber U (1994) An active Mehler-peroxidase reaction sequence can prevent cyclic PS I electron transport in the presence of dioxygen in intact spinach chloroplasts. Photosynth Res 41: 429-437

Klughammer C, Schreiber U (2008) Saturation Pulse method for assessment of energy conversion in PS I. PAN 1: 11-14 (see http://www.walz.com)

Mano J, Miyake C, Schreiber U, Asada K (1995) Photoactivation of electron flow from NADPH to plastoquinone in spinach chloroplasts. Plant Cell Physiol 36: 1589-1598

Mi H, Klughammer C, Schreiber U (2000) Light-induced dynamic changes of NADPH-fluorescence in *Synechocystis* PCC 6803 and its *ndhB* defective mutant M55. Plant Cell Physiol 41: 1129-1135

Olson JM (1958) Fluorometric identification of pyridine nucleotide changes in photosynthetic bacteria and algae. Brookhaven Symposia in Biology 11: 316-324

Renger G, Schreiber U. (1986) Practical applications of fluorometric methods to algae and higher plant research. In: Light Emission by Plants and Bacteria. Govindjee, Amesz J and Fork DC, eds, pp 587-619. New York, Academic Press

Schreiber U, Endo T, Mi H, Asada K (1995) Quenching analysis of chlorophyll fluorescence by the saturation pulse method: particular aspects relating to the study of eukaryotic algae and cyanobacteria. Plant Cell Physiol 36: 873-882

Schreiber U, Klughammer C (2008) New accessory for the Dual-PAM-100: The P515/535 module and examples of its application. PAN 1: 1-10
(see http://www.walz.com)

Schreiber U, Schliwa U, Bilger W (1986) Continuous recording of photochemical and non-photochemical chlorophyll fluorescence quenching with a new type of modulation fluorometer. Photosynth Res 10: 51-62

Schreiber U, Vidaver W (1974) Chlorophyll fluorescence induction in anaerobic *Scenedesmus obliquus*. Biochim Biophys Acta 386: 97-112

Schreiber U, Vidaver W (1975) Analysis of anaerobic fluorescence decay in *Scenedesmus obliquus*. Biochim Biophys Acta 387: 37-51

Schuldiner S, Rottenberg H, Avron M (1972) Determination of ΔpH in chloroplasts. 2. Fluorescent amines as a probe for the determination of ΔpH in chloroplasts. Eur J Biochem 25: 64-70

Takahama U, Shimizu-Takahama M, Heber U (1981) The redox state of the NADP system in illuminated chloroplasts. Biochim Biophys Acta 637: 530-539

Teuber M, Rögner M, Berry S (2001) Fluorescent probes for non-invasive bioenergetic studies of whole cyanobacterial cells. Biochim Biophys Acta 1506: 31-46

Tillberg J, Giersch C, Heber U (1977) CO_2 reduction by intact chloroplasts under diminished proton gradient. Biochim Biophys Acta 461: 31-47